Davydov soliton dynamics: temperature effects

1991 J. Phys.: Condens. Matter 3 4333

(http://iopscience.iop.org/0953-8984/3/24/003)

J. Phys.: Condens. Matter 3 (1991) 4333–4348. Printed in the UK

Davydov soliton dynamics: temperature effects

Wolfgang Förner
Department of Theoretical Chemistry, Friedrich Alexander University, Erlangen-Nürnberg, Egerlandstrasse 3, W-8520 Erlangen, Federal Republic of Germany

Received 28 September 1990, in final form 31 January 1991

Abstract. With an improved version of our model for inclusion of temperature into Davydov's model using the $|D_2\rangle$ *ansatz* state we surveyed the parameter space of the Hamiltonian. Solitons were found to be stable at 300 K under certain conditions on the parameter values which may be fulfilled in proteins. It is numerically shown that our results agree with those of special versions of Langevin-equation models. Also agreement with recently published perturbation theoretical results is found.

1. Introduction

For the explanation of a wide variety of chemical and physical phenomena the introduction of non-linear forces has turned out to be necessary (see [1] and references therein for a short list). Many biological processes are associated with an energy transfer through proteins, where this energy is released by hydrolysis of adenosine triphosphate (ATP). The mechanism of this energy transport is not quite clear [2]. As an alternative to electronic mechanisms [2], one can assume that the energy is stored as vibrational energy in the C=O stretching mode (amide-I) of a polypeptide chain. Following Davydov's idea [3], one can take into account the coupling between the amide-I vibration and the acoustic phonons in the lattice. Through this coupling, non-linear terms appear in the equations of motion. In this way the energy can be transported as a localized wave packet in solitary waves. Direct experimental evidence for the existence of such solitons in proteins is still missing. This is due to the complex structure of proteins, which makes such measurements very difficult. However, in acetanilide crystals a substructure with chains of hydrogen bonds similar to proteins is present. In low-temperature infrared and Raman spectra of these materials a new band in the amide-I region appears. Up to now this band could only be explained with the help of a model similar to the Davydov soliton concept in proteins [4]. However, in this case the amide-I vibration is coupled to optical phonons and the soliton is pinned.

Since Davydov's [5] result that solitons are stable at $T \simeq 300$ K, which he obtained via analytical considerations, there has been considerable discussion on this point in the literature. Halding and Lomdahl [6] found stable pulses at $T = 310$ K in classical molecular dynamics studies on peptide units moving in a Lennard–Jones potential. Lomdahl and Kerr [7] and Lawrence *et al* [8] used the $|D_2\rangle$ *ansatz* together with a damping and a noise term to introduce temperature. They found stable solitons only for $T \simeq 10$ K. However, Bolterauer [9] argued that their classical thermalization scheme

0953-8984/91/244333 + 16 $03.50

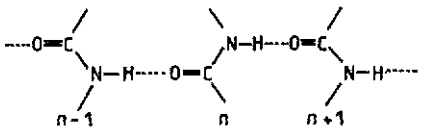

Figure 1. Schematic picture of a hydrogen-bonded channel in a protein.

should lead to incorrect results when applied to a quantum system. Bolterauer [9] and other workers (see references in [9]) found solitons to be stable at $T \simeq 300$ K. Cruzeiro *et al* [10] derived a thermally averaged Hamiltonian and evolution equations using the $|D_1\rangle$ *ansatz*. They also found stable solitons at 300 K. Very recently Cottingham and Schweitzer [11] found a lifetime of only about 1 ps for the soliton at 300 K using perturbation theory. Wang *et al* [12] found solitons to be stable up to about 7 K with the help of quantum Monte Carlo simulations.

In this paper the model used in our previous works [13, 14] is worked out and applied within a wide range of parameters (section 2). In this model we populate the normal modes of the lattice according to the temperature under consideration (Bose–Einstein distribution). After lattice equilibration the soliton is started in the thermalized lattice. In section 3 we compare several versions of a Langevin-equation model with each other and with ours. In Langevin-equation models it is assumed that the system transfers energy to its degrees of freedom which are not explicitly treated and function as a heat bath. This energy transfer is modelled by a damping term. The external degrees of freedom transfer energy back in a random manner, modelled by a random force term. Section 4 deals with perturbation theory results following [11]. In [11] the Hamiltonian is partially diagonalized such that the $|D_2\rangle$ soliton is an exact eigenstate of the diagonal part. The off-diagonal part is treated as perturbation. Then one can compute the transition probability from a state with a $|D_2\rangle$ soliton plus a thermally averaged phonon distribution to a final state containing only phonons by first-order perturbation theory. In this way the lifetime of $|D_2\rangle$ solitons can be obtained. Finally in section 5 the results are summarized.

2. Heat bath model and soliton dynamics

The Hamiltonian used for this study is in the most simple form for the system investigated in [3]. More sophisticated forms of the Hamiltonian which incorporate more details of the protein structure have led qualitatively to the same results [15]:

$$\hat{H} = \sum_n \left(E_0 \hat{b}_n^+ \hat{b}_n - J(\hat{b}_n^+ \hat{b}_{n+1} + \hat{b}_{n+1}^+ \hat{b}_n) + \frac{\hat{p}_n^2}{2M} + \frac{W}{2}(\hat{q}_n - \hat{q}_{n-1})^2 + X\hat{b}_n^+ \hat{b}_n(\hat{q}_n - \hat{q}_{n-1}) \right). \tag{1}$$

In equation (1), $\hat{b}_n^+$ and $\hat{b}_n$ are the usual boson creation and annihilation operators respectively [15] for the amide-I oscillators at sites n (figure 1).

From infrared spectra the ground-state energy of an isolated amide-I oscillator can be deduced (E_0 0.205 eV) [16]. Usually for all parameters in equation (1), site-independent mean values are used. The average value for the dipole–dipole coupling

between neighbouring amide-I oscillators is $J = 0.967$ meV [16]. The average spring constant of the hydrogen bonds is usually taken to be $W = 13\ \mathrm{N\ m^{-1}}$ [16]. In our preliminary paper [13] we used $W = 76\ \mathrm{N\ m^{-1}}$ which is the spring constant for the hydrogen bonds in the hydrogen carbonate dimer [17]; $\hat{p}_n$ is the momentum and $\hat{q}_n$ the position operator of unit n. The average mass M is taken as that of myosine ($M = 114m_p$ where m_p is the proton mass) [16]. The energy of the CO stretching vibration in hydrogen bonds is a function of the length r of the hydrogen bond ($E = E_0 + Xr$) [18]. For X the experimental value is 62 pN [16]. *Ab initio* calculations on formamide dimers usually lead to $X = 30$–50 pN [19].

For the solution of the time-dependent Schrödinger equation we used the displaced oscillator state *ansatz* ($|D_2\rangle$) [3]. In [3, 5] the expectation values of the Hamiltonian (1) with $|D_2\rangle$ was formed and this expectation value was used as the classical Hamiltonian function. In this way Davydov obtained the equations of motion. Kerr and Lomdahl [20] have shown that these equations can be obtained also by purely quantum mechanical methods and also for states of more than one quantum [21]. Explicit forms of the equations of motion used can be found in [1].

In the case of Davydov's more sophisticated $|D_1\rangle$ states the optimized equations of motion can only be obtained by quantum mechanical methods [22, 23]. Here Davydov's [5] method leads to different equations which do not reproduce the exactly soluble transportless case ($J = 0$) of (1) as shown by Brown *et al* [24–26], while the optimized $|D_1\rangle$ equations do [22, 23]. The $|D_2\rangle$ state reproduces the lattice dynamics for $J = 0$ correctly but leads to an incorrect phonon energy [24–26]. Since $|D_2\rangle$ results can be mapped onto the results of the partial dressing theory of Brown and Ivic [27] and only the energies are incorrect, we decided to use the $|D_2\rangle$ equations for our calculations.

In practical calculations on chains of N units we added an additional potential term $V' = W'(q_1 + q_N)$ with $W' = 100W$ to (1) in order to keep the chain ends fixed. For the inclusion of temperature we first solve the decoupled lattice problem ($X = 0$) [28], which is simply a chain of coupled harmonic oscillators. As initial excitations we distribute an energy of Nk_BT (where k_B is Boltzmann's constant) on the normal modes using Bose–Einstein statistics. Half of this energy was distributed as potential energy and the other half as kinetic energy. Thus the lattice displacements at a given time t_0 are

$$\bar{q}_n(t_0) = \sum_k V_{nk} \frac{\gamma_k}{\omega_k} \sin(\omega_k t_0 + \varphi_k)$$
$$\dot{\bar{q}}_n(t_0) = \sum_k V_{nk} \gamma_k \cos(\omega_k t_0 + \varphi_k) \tag{2}$$

where the initial displacements and momenta are contained in γ_k and φ_k:

$$\varphi_k = \sin^{-1}\left(\frac{\omega_k}{\gamma_k} \sum_n V_{nk} q_n(0)\right)$$
$$\gamma_k = \left[\omega_k^2 \left(\sum_n V_{nk} q_n(0)\right)^2 + \left(\sum_n V_{nk} \dot{q}_n(0)\right)^2\right]^{1/2}. \tag{3}$$

Here ω_k are the eigenfrequencies and $\mathbf{V}$ contains the eigenvector coefficients of the decoupled chain. The time t_0 can be chosen arbitrarily. The results of soliton dynamics do not depend on the choice of t_0 as we have shown in [14]. However, since t_0 is the time actually used for lattice equilibration, it should be kept explicitly to ensure that the

reported calculations are fully reproducible. At t_0 with the thermally equilibrated lattice we introduce a vibrational quantum at a given site n_0 (usually we use $N = 200$, $n_0 = 199$ and $t_0 = 120$ ps).

Now $q_n(t + t_0)$ can be decomposed into two parts:

$$q_n(t + t_0) = Q_n(t) + \bar{q}_n(t + t_0) \tag{4}$$

where $Q_n(0) = 0$ and

$$\bar{q}_n(t + t_0) = \sum_k V_{nk} \frac{\gamma_k}{\omega_k} \sin[\omega_k(t + t_0) + \varphi_k]. \tag{5}$$

Using $M\ddot{\bar{q}}_n = W(\bar{q}_{n+1} - 2\bar{q}_n + \bar{q}_{n-1})$ the equation of motion for Q_n is

$$M\ddot{Q}_n = W(Q_{n+1} - 2Q_n + Q_{n-1}) + X(|a_{n+1}|^2 - |a_n|^2). \tag{6}$$

Now one performs a phase transformation on a_n:

$$a_n = b_n \exp\left(-\mathrm{i}\frac{X}{\hbar}\int_{t_0}^{t+t_0} (\bar{q}_n - \bar{q}_{n-1})\,\mathrm{d}t'\right) = b_n \exp\left(\frac{-\mathrm{i}Xf_n}{\hbar}\right) \tag{7}$$

with

$$f_n = -\sum_k (V_{nk} - V_{n-1,k}) \frac{\gamma_k}{\omega_k^2} \{\cos[\omega_k(t + t_0) + \varphi_k] - \cos(\omega_k t_0 + \varphi_k)\}. \tag{8}$$

Thus we obtain finally

$$\mathrm{i}\hbar\dot{b}_n = -J\{b_{n+1} \exp[-\mathrm{i}(X/\hbar)g_n] + b_{n-1} \times \exp[+\mathrm{i}(X/\hbar)g_{n-1}]\} + X(Q_n - Q_{n-1})b_n \tag{9}$$

where

$$g_n = f_{n+1} - f_n \tag{10}$$

and

$$M\ddot{Q}_n = W(Q_{n+1} - 2Q_n + Q_{n-1}) + X(|b_{n+1}|^2 - |b_n|^2). \tag{11}$$

Note that, for $t = t_0$, $f_n(t_0) = 0$ and thus $b_n(t_0) = a_n(t_0)$. $|a_n(t + t_0)|^2 = |b_n(t + t_0)|^2$ holds anyway. Note further that $Wg_n = \Delta\bar{p}_n(t + t_0) = \bar{p}_n(t + t_0) - \bar{p}_n(t_0)$ is the change in momentum of unit n due only to thermal motion.

As equation (9) shows, the heat bath introduces two oscillating phase factors at J. These oscillations occur in both space and time. The spatial oscillation is due to the normal mode coefficients V_{nk}. With increasing temperature the admixture of higher normal modes increases, which have more spatial oscillations owing to their larger number of nodes. Thus temperature has the same net effect as disorder in the site energy E_0 which can be traced back to exactly the same mathematical structure [1]. However, in addition we also have oscillations in time which become faster with increasing temperature owing to the higher frequencies (ω_k) which become more important. Since the phases at J are proportional to the coupling constant X, one expects a threshold value for X. If X becomes larger than this threshold, the soliton should be destroyed. However, its value has to be determined numerically.

Since in our model only a phase at J occurs, this phase factor cannot be viewed as an analogue to the Debye–Waller factor found in $|D_1\rangle$ theories [5, 10]. In these cases the

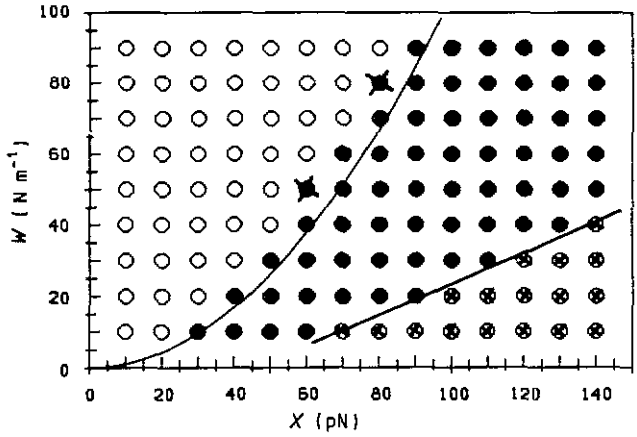

Figure 2. Survey of the $[W, X]$-parameter space at $J = 0.967$ meV and $T = 0$ K for $|D_2\rangle$ dynamics for a one-site excitation: ○, dispersive; ✱, dispersive solitary wave travelling slowly; ●, travelling soliton; ⊗, pinned soliton; ——, function given in equation (12).

exponent contains a real part and thus J is scaled to lower values. However, Scott [29] argues that probably one should introduce an additional Debye–Waller factor into the $|D_2\rangle$ theory also. A possible way to introduce a Debye–Waller factor into $|D_2\rangle$ theory could be to use the factor occurring in $|D_1\rangle$ or partial dressing theory and remove its site dependence. However, it is questionable whether such a procedure would be consistent. In the following sections we shall compare the results of our above-described model also with those of other methods to treat temperature. These methods will be described in the appropriate sections.

As mentioned above, we used $a_n(0) = \delta_{n,199}$ in a chain of 200 units as initial conditions. For the numerical solution of the equations of motion a Runge–Kutta method correct up to fourth order in the time step τ was applied [30]. Using a time step of $\tau = 1$ fs and $T = 300$ K each of the simulations through 120 ps required roughly 850 CPU s on a CDC Cyber 995 E computer. The norm remained constant up to about 10^{-6} and the total energy error was less than 0.6% of its initial value. A possible (owing to numerical errors) imaginary part of the total energy remained zero within 10^{-18} eV.

For comparison we show in figure 2 the results at zero temperature and $J = 0.967$ meV. The full curve corresponds to the formula

$$W = (16/\pi^2 J)X^2 \tag{12}$$

which gives the threshold for travelling solitons in zero-temperature continuum theory [29]. Each circle represents a simulation performed. The results show that the continuum theory formula (12) is well reproduced by our numerical study. The threshold for pinning shows a linear curve. A surprising observation was made for $W = 10$ N m^{-1} with $X =$ 100, 110, 120 and 130 pN. In those cases besides the pinned soliton a travelling small-amplitude soliton is emitted.

In figure 3 the results of our simulations are shown for $J = 0.5, 0.7, 0.9$ and 1.1 meV in the same way as figure 2 for $T = 300$ K.

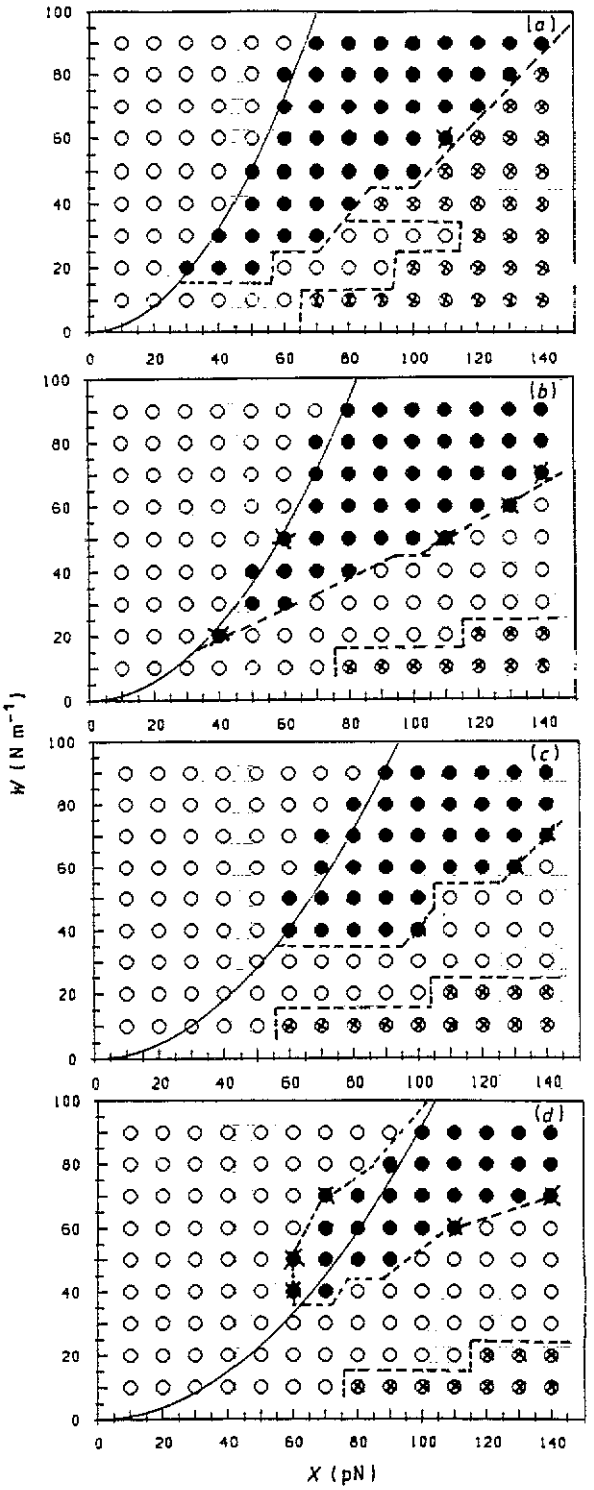

Figure 3. Same as figure 2 but at $T = 300$ K with our heat bath model for (*a*) $J = 0.5$ meV, (*b*) $J = 0.7$ meV, (*c*) $J = 0.9$ meV and (*d*) $J = 1.1$ meV.

First of all one recognizes that the zero-temperature continuum limit curve (12) still agrees fairly well with the threshold X_1 for the formation of travelling solitons. This observation in connection with previous results [14] was first made by Scott [29]. The agreement, however, is best for small values of J and fairly good up to $J = 0.967$ meV, while for $J = 1.1$ meV it is worse. However, as discussed already in [14] for $T = 300$ K there is a second threshold X_2. For $X > X_2$ the travelling solitons are destroyed by thermal fluctuations. Since $X_2(W)$ intersects $X_1(W)$, we also have a threshold value for W below which no travelling solitons are possible. We find this value to be 20 N m^{-1} for $J = 0.5$ meV, 30 N m^{-1} for $J = 0.7$ meV, and 40 N m^{-1} for $J = 0.9$ meV and also for $J = 1.1$ meV. However, since for $X_2(W)$ no analytical form is known, these values can only be determined numerically. In general, the smaller J, the larger the stability region of travelling solitons becomes. This is to be expected physically, since J is responsible for the dispersion of the excitation.

In addition a third threshold $X_3(W)$ occurs such that for $X > X_3$ a pinned solitary wave occurs. For large values of W, X_2 and X_3 coincide and no dispersion can be observed. Physically for $W > W_t$ (W_t is the soliton threshold for W) if $X < X_1$ the non-linearity is not strong enough to prevent the dispersion of the initial excitation. For $X_1 < X < X_2$ the non-linearity is strong enough for this purpose and a travelling soliton results. However, since the thermal fluctuations enter the equations of motion for a_n in a term proportional to X, dispersion occurs again for $X_2 < X < X_3$. Then the fluctuations in the term $X(q_n - q_{n-1})a_n$ are large enough to destroy the soliton. Finally, for $X > X_3$ a pinned soliton occurs which disperses very slowly into the chain. W_t occurs because, if W is small, the displacements $q_n - q_{n-1}$ must be large to accommodate a potential energy $\frac{1}{2}Nk_BT$ in the lattice. These large displacements interfere with the soliton and are then able to destroy it.

Brizhik *et al* [30] found from continuum theory that for an initial excitation located at site n_0 and given by

$$a_n = A \operatorname{sech}[(n - n_0)X^2/4JW] \tag{13}$$

the threshold for soliton formation should be at $X = 0$. A is a normalization factor. Thus it seems to be interesting to study this case too. In figure 4(a) we show for $J = 0.967$ meV the case $T = 0$. Points in circles indicate here computations where the width of the pulse is too large to allow meaningful simulations within a chain of 200 units. $n_0 = 199$ was used in the case of figure 4. That implies that a soliton threshold of $X = 0$ does not mean too much since for small X the initial pulse is already broader than 200 units. In the small-X region, rather broad solitary waves occur. They move very slowly away from $n_0 = 199$ and tend to stop after a couple of units. In addition they disperse slowly. Crossed black circles in this region mark cases where the waves are not fully dispersed after 120 ps. Real solitons show up for X-values larger than in the case of a one-site excitation. In the region of large X and small W the pulse (13) is so small that it can be already considered as a one-site excitation. The soliton thresholds are linear in this case. In figure 4(b) we show the $T = 300$ K case. Obviously the region of travelling solitons is much smaller than for the one-site excitation. The region with extremely slowly moving dispersive solitary waves is smaller than for $T = 0$ as expected. An explanation for this phenomenon is still missing. If one centres the pulse at $n_0 = 150$ (figure 4(c)), the picture becomes irregular. However, the region where solitons occur is larger. In our opinion an initial sech pulse is somewhat artificial. There is no physical reason why energy released by hydrolysis of ATP should excite the amide-I oscillators with a preformed soliton shape. To us an initial one- or two- site excitation seems to be far more probable.

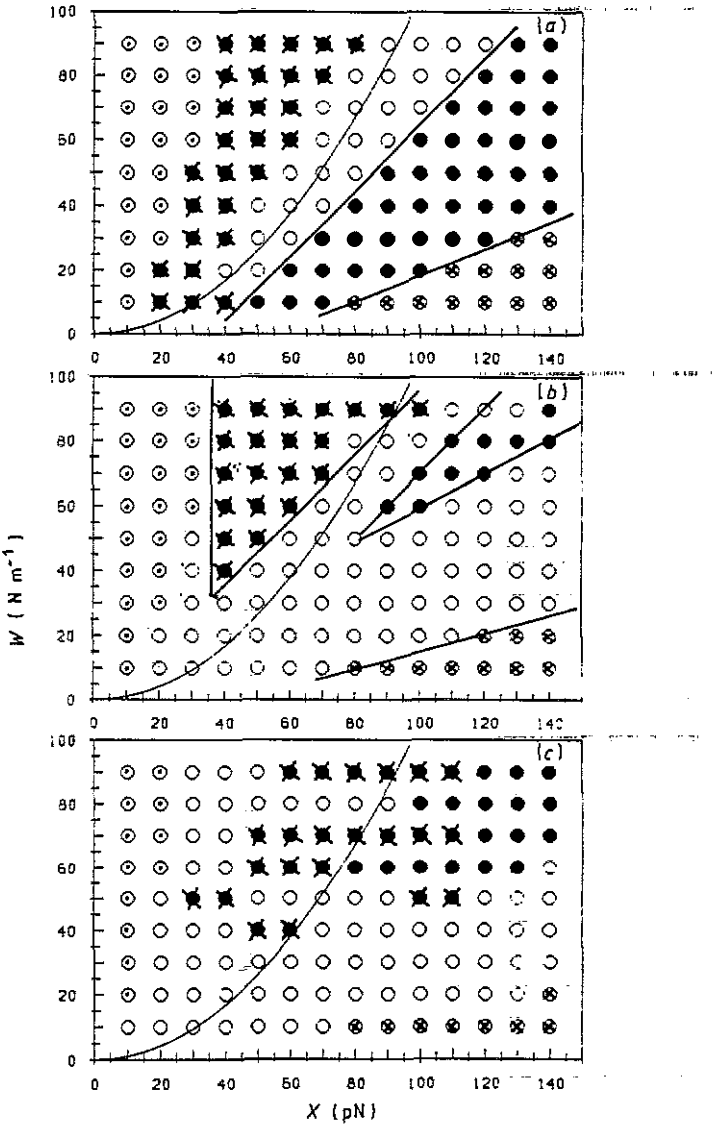

Figure 4. Same as figure 2 with our heat bath model for (*a*) $T = 0$ K, sech pulse at $n_0 = 199$, (*b*) $T = 300$ K, sech pulse at $n_0 = 199$, and (*c*) $T = 300$ K, sech pulse at $n_0 = 150$. Here ⊙ indicates parameter values where such a pulse is spread over the complete chain and thus a 200-unit chain allows no meaningful simulation.

3. Langevin equation

In the Langevin *ansatz* for the treatment of temperature as reported by Halding and Lomdahl [6] and Lomdahl and Kerr [31] a damping term and a random force term is added to the equations of motion:

$$i\hbar\dot{a}_n = -J(a_{n+1} \pm a_{n-1}) + X(q_n - q_{n-1})a_n \tag{14a}$$

$$M\ddot{q}_n = W(q_{n+1} + 2q_n + q_{n-1}) + X(|a_{n+1}|^2 - |a_n|^2) - M\Gamma\dot{q}_n + F_n(t). \tag{14b}$$

Using as correlation function

$$\langle F(x,t)F(0,0)\rangle = 2Mk_B T\Gamma\delta(x)\delta(t)/a \tag{15}$$

(a is the lattice constant) (14*b*) becomes a Langevin equation. The random forces are assumed to follow a normal distribution with standard deviation $\sqrt{\sigma}$:

$$W(F_n) = (1/\sqrt{2\pi\sigma})\exp(-F_n^2/2\sigma). \tag{16}$$

In actual computations we computed a series of $L = 12$ random numbers $X_{nr}(t)$ $(0 \leqslant X_{nr}(t) \leqslant 1)$ for each site at each time step t and generated the forces as

$$F_n(t) = \sqrt{\sigma}\sum_{r=1}^{L}[X_{nr}(t) - \tfrac{1}{2}]. \tag{17}$$

Thus the variance of $X_{nr}^{(t)} - \frac{1}{2}$ is $\frac{1}{12}$ and the standard deviation of $F_n^{(t)}$ is $\sqrt{\sigma}$, with its mean value 0 as required. The interval for the random forces is $|F_n^{(t)}| \leqslant 6\sqrt{\sigma}$. Thus (17) represents an approximate Gaussian distribution which would be exact for $L \to \infty$. The effect of the two additional terms is to drive the system into thermal equilibrium with a time constant Γ. Requiring the random force to be constant within a time step τ we obtain

$$\sigma = 2Mk_B T\Gamma/\tau. \tag{18}$$

Γ is the inverse time constant of the heat bath. If Γ is large, the heat bath is fast and vice versa. In our actual simulations in this case we fixed units 1 and N ($N = 200$) at $q_1 = q_N = 0$ and we used $\tau = 5$ fs. For a typical simulation the norm is conserved up to 10^{-4} in 120 ps. Halding and Lomdahl [6] and Lomdahl and Kerr [31] worked with two models at the standard set of parameters only. They chose $\Gamma = \nu_{min}$, where ν_{min} is the lowest (non-zero) frequency of the lattice. For a chain of 100 units, $W = 13$ N m^{-1} and $M = 114$ M_p, the lowest phonon frequency is $\omega_0 = 0.2594$ ps^{-1}, leading to $\nu_{min} = 0.041\,28$ ps^{-1} or $\nu_{min} = 0.005\sqrt{W/M}$. For 200 units we obtain $\omega_0 = 0.1297$ ps^{-1} and $\Gamma = \nu_{min} = 0.020\,46$ ps^{-1}. Thus the heat bath has the same time constant as the slowest vibration of the lattice.

In model I they equilibrated the decoupled lattice until

$$\left\langle \sum_n \tfrac{1}{2}M\dot{q}_n^2(t) \right\rangle = \tfrac{1}{2}Nk_B T \tag{19}$$

is achieved and thus the lattice is equilibrated. Then the heat bath is switched off and the soliton started. This model should give similar results to ours. In model II they switched on the heat bath and the soliton dynamics simultaneously. However, this corresponds to an amide-I excitation in a lattice with a zero-temperature equilibrium structure. We believe that model I and ours are more physical, since in these cases the soliton is started in a thermally equilibrated lattice, a situation which should be closest to reality. Finally we introduce a model III, where we first equilibrate the lattice but, after the soliton has been started, the heat bath is not switched off. Model I and ours should be reasonable if the heat bath is slow compared with the soliton velocity, while model III should be the best if the actual value of Γ is of importance.

For comparison with the results of [6, 31] note that we used the asymmetric exciton–phonon interaction while [6, 31] use the symmetric interaction. However, the structure (figure 1) suggests that an asymmetric interaction is realistic. In the symmetric interaction

model the $C = 0$ oscillator n would interact with the hydrogen bond in which it takes part with the same strength as with the hydrogen bond between units n and $n + 1$ in which it does not take part. Estimates show that the coupling constant for the latter interaction is an order of magnitude smaller than that for the former, and thus the latter interaction can be neglected [15]. For comparison we show in figure 5(*a*) the results of an $[X, W]$ parameter space survey at $J = 0.967$ meV, $T = 300$ K, using our model. One simulation using Langevin equations used typically 100 CPU s for model I, 700 CPU s for model II, and 1500 CPU s for model III on our Cyber 995E computer. In figure 5(*b*) we show the results obtained with model I and $\Gamma = \nu_{\min}$. As we expected, figures 5(*a*) and 5(*b*) are very similar and the two models agree with each other. In the region of the parameter values used in [6, 31] we find no soliton, in complete agreement with [6, 31].

Using model II for all parameter sets in figure 5(*b*) we found no trace of a soliton or a solitary wave, again in agreement with [6, 31]. However, as explained above, we consider model II as rather unphysical. In model I, Γ is not important, because the lattice is equilibrated before the soliton start and the heat bath is switched off afterwards. In model II we expect that for decreasing Γ the results should approach the zero-temperature situation since, if the heat bath becomes very slow, it simply has not enough time to disturb the soliton. In figure 5(*c*) we show the results for model III using $\Gamma = 0.1\nu_{\min}$. As is obvious for the slow heat bath we obtain results which are in rough agreement with ours and those of model I. In figure 5(*d*), $\Gamma = \nu_{\min}$ is used. We see that the region of soliton stability is shifted to smaller X-values. Obviously the faster heat bath requires a smaller interaction of the lattice fluctuations with the oscillators to allow a travelling soliton. Using a still faster heat bath ($\Gamma = 10\nu_{\min}$) not shown in figure 5, the region of stable travelling solitons vanishes completely. Only pinned solitons are still found.

Thus our model agrees with Langevin model I and with model III if in the latter case the heat bath is not too fast ($\Gamma \leqslant \nu_{\min}$). However, concerning Langevin-equation models the point made by Bolterauer [9] still holds. He uses the simple model of two coupled harmonic oscillators and treats them both quantum mechanically on the one hand, and one quantum mechanically and the other classically on the other hand. He finds that in the adiabatic treatment the energy transferred into the quantum oscillator is too large compared with the exact treatment. He concludes [9] that thus in Langevin models the effects of thermal fluctuations on the soliton may be overestimated.

4. Perturbation theory

A very appealing model for treating temperature effects on Davydov solitons was recently introduced by Cottingham and Schweitzer [11]. They [11] could diagonalize the Hamiltonian partially. Then one can define $\hat{H} = \hat{H}_0 + \hat{V}$ where $\hat{H}_0$ is the diagonal part of $\hat{H}$ and $\hat{V}$ the non-diagonal part. Thus $\hat{V}$ can be treated as a perturbation. Furthermore the Davydov soliton state ($|D_2\rangle$) is an exact eigenstate of $\hat{H}_0$ and thus first-order perturbation theory using $\hat{V}$ as perturbation allows one to calculate the soliton lifetimes. They could compute the transition probability from an initial state containing a Davydov soliton and a thermal distribution of phonons to a final state without the soliton. From this probability they could derive an explicit expression for the lifetime of a pinned soliton.

To compare our model with that of Cottingham and Schweitzer [11] we took a cyclic chain as in [11] where only pinned solitons are found numerically [28]. We used $W =$

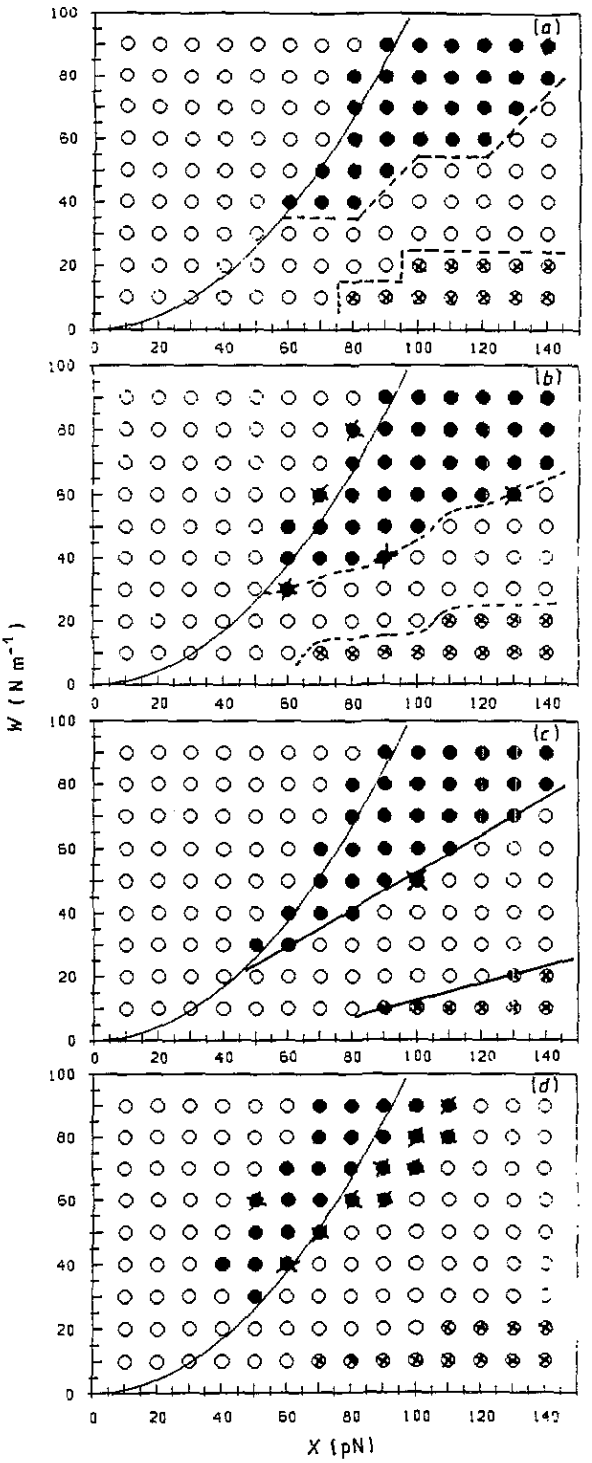

Figure 5. Same as figure 2 for $J = 0.967$ meV at $T = 300$ K computed with (*a*) our heat bath model, (*b*) Langevin-equation model I, $\Gamma = \nu_{mm}$, (*c*) Langevin-equation model III, $\Gamma = 0.1\nu_{min}$, and (*d*) Langevin-equation model III, $\Gamma = \nu_{min}$.

13 N m, $X = 62$ pN and $a_n(0) = A\ \mathrm{sech}[(n - 100)X^2/WJ]$ as initial condition as in [11]. In addition we implemented the symmetric interaction into our program for the purpose of comparison, since in [11] this model was used. As shown in [20], the two interaction models lead to rather different results. For comparison we varied J and estimated soliton lifetimes from our model. For this purpose the initial excitation was placed at site 100 and we used the soliton detector plot in [6, 31]. In this plot each point in the (n, t) plane where $|a_n(t)|^2 > 0.02$ and $q_{n+1} - q_{n-1} < 0$ (the typical soliton conditions) coincide is marked. The case $J = 0.967$ meV is shown as an example in figure 6(*a*). The plot shows that this kind of presentation is not suitable to estimate soliton lifetimes.

The exciton part of the numerically computed wave function is

$$|\phi(t)\rangle = \exp(-\mathrm{i}Et/\hbar) \sum_n a_n(t)\hat{a}_n^+ |0\rangle \tag{20}$$

$$E = E_0 + \tfrac{1}{2} \sum_n [p_n^2/M + W(q_n - q_{n-1})^2]. \tag{21}$$

Further, the exciton part of the solution of $\hat{H}_0$ for soliton velocity $v_s = 0$ is given by [11]

$$|D_2\rangle = \exp(-\mathrm{i}\bar{E}t/\hbar)A \sum_n \mathrm{sech}[(n - n_0)X^2/WJ]\hat{a}_n^+ |0\rangle \tag{22}$$

$$\bar{E} = E_0 - 2J - W^2J^3/3X^4. \tag{23}$$

Thus we can easily compute

$$\langle D_2|\phi(t)\rangle = \exp(\mathrm{i}\Delta t/\hbar)A \sum_n a_n(t)\mathrm{sech}[(n - n_0)X^2/WJ] \tag{24}$$

$$\Delta = -2J - W^2J^3/3X^4 - \tfrac{1}{2} \sum_n [p_n^2/M + W(q_n - q_{n-1})^2] \tag{25}$$

and the weight of the initial soliton state in the exciton part of the wave function is $w(t) = |\langle D_2/\Phi(t)\rangle|$. Figures 6(*b*) and (*c*) show two examples of $w(t)$ for long time simulations with $J = 0.2$ and 0.3 meV. As an indicator for the soliton lifetime we take the last maximum of $w(t)$ before the steep descent to 0.5 or below, which occurs for each J value considered. For the actual estimation of lifetimes we have recalculated the dynamics through a smaller time appropriate for each value of J (double the soliton lifetime from perturbation theory). However, one has to keep in mind that, from dynamical simulations, only estimates can be obtained.

In table 1 we show the lifetimes (τ_1) obtained with our model at 300 K and the lifetimes (τ_2) computed with equation (31) of [11] for some values of J. Our program for computation of τ_2 was checked by reproducing the results given in [11]. In figure 7 the results are plotted to facilitate comparison. Obviously the two models agree very well and the decrease in soliton lifetimes with increasing J is certainly correct since J governs the dispersion and $J = 0$ is simply the transportless case.

5. Conclusion

We have studied the soliton stability at $T = 300$ K within a wide range of parameter values and in different models. We found agreement of our model with Langevin models, provided that the heat bath is not too fast compared with the soliton. Our model agrees at least qualitatively also with perturbation theoretical results. For further justification

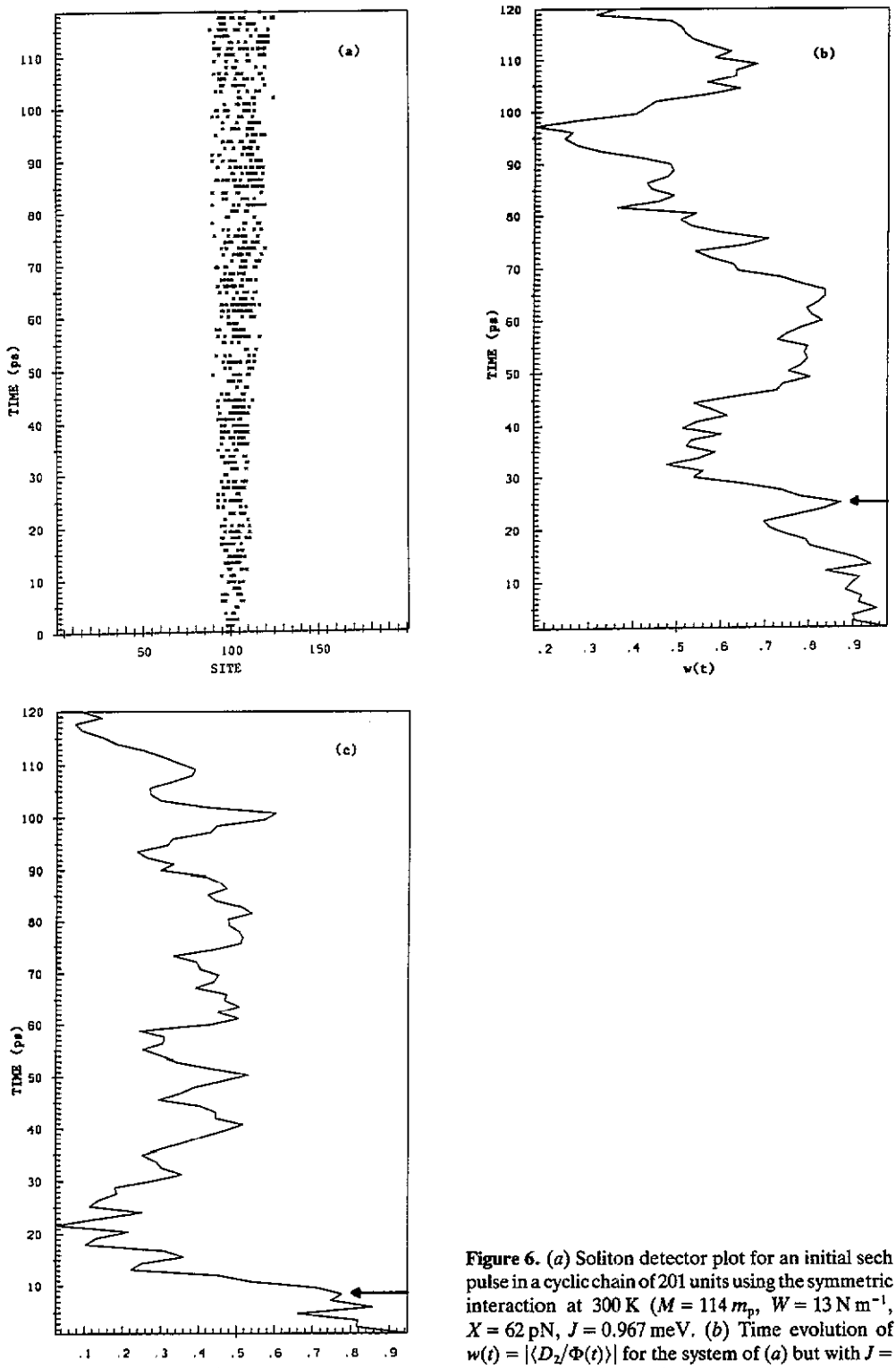

Figure 6. (*a*) Soliton detector plot for an initial sech pulse in a cyclic chain of 201 units using the symmetric interaction at 300 K ($M = 114\,m_p$, $W = 13\,\mathrm{N\,m^{-1}}$, $X = 62$ pN, $J = 0.967$ meV. (*b*) Time evolution of $w(t) = |\langle D_2/\Phi(t)\rangle|$ for the system of (*a*) but with $J = 0.2$ meV. (*c*) Same as (*b*) for $J = 0.3$ meV.

Table 1. Lifetimes of a pinned soliton in a cyclic chain of 200 units with a sech pulse as initial condition at 300 K ($W = 13$ N m^{-1}; $X = 62$ pN; $M = 114m_p$) as estimated from our model (τ_1) and calculated from perturbation theory [20] (τ_2) as function of J.

J (meV)	τ_1 (ps)	τ_2 (ps)
0.0	∞	∞
0.1	96.0	207.91
0.2	25.0	24.58
0.3	8.2	8.14
0.4	3.8	3.95
0.5	2.6	2.34
0.6	1.6	1.56
0.7	1.5	1.13
0.8	1.1	0.87
0.9	0.7	0.69
1.0	0.6	0.58

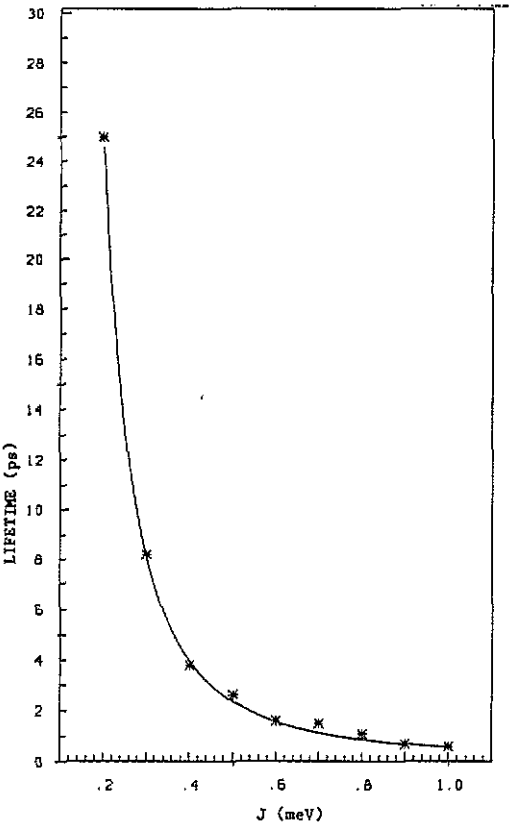

Figure 7. Soliton lifetime τ_0 as function of J computed with the Cottingham–Schweitzer formula (——) and as estimated from our model (*).

of our model the extension of the recently published quantum Monte Carlo simulations [12] to parameter values where we find stable solitons at $T = 300$ K would be desirable.

However, based on the above given comparisons, we are confident that our basic conclusion of soliton stability in a parameter region $W > 40$ N m^{-1} and $X > 50$–60 pN should be model independent. The values of X for proteins found in the literature are roughly in this range (experimental value $X = 62$ pN). The usually quoted value of $W = 13$ N m^{-1} is certainly too small to allow soliton formation. However, as already discussed before [14], a value of W taken from crystalline formamide [32] is certainly too low. In formamide, free molecules vibrate while, in proteins, vibration of a hydrogen bond requires distortions of the covalent backbone of the α-helix. Thus an effective spring constant for this vibration should be larger than the formamide value. For a clear decision of whether the Davydov mechanism in proteins can function, first of all realistic parameter values have to be established. Attempts based on *ab initio* calculations are in progress [33]. Further, the existing models for treating temperature effects should be compared, especially their dependence on the parameter values. Finally one has to mention that there is still no quantitative information available about the errors introduced by the different *ansatz* states used in the literature.

Acknowledgments

The financial support of the Fonds der Chemischen Industrie, the National Foundation for Cancer Research and the Deutsche Forschungsgemeinschaft (project Ot 51/6-2) is gratefully acknowledged.

References

[1] Förner W 1991 *J. Phys.: Condens. Matter* **3** 19 3235–54
[2] Szent-Györgyi A 1941 *Nature* **148** 157; 1941 *Science* **93** 609
Bakhshi A K, Otto P, Ladik J and Seel M 1986 *Chem. Phys.* **20** 683
[3] Davydov A S and Kislukha N I 1973 *Phys. Status. Solidi* b **59** 465
Davydov A S 1979 *Phys. Scr.* **20** 387; 1982 *Sov. Phys.–Usp.* **25** 898; 1982 *Biology and Quantum Mechanics* (Oxford: Pergamon)
[4] Careri G, Buontempo U, Galuzzi F, Scott A C, Gratton E and Shyamsunder E 1984 *Phys. Rev.* B **30** 4689
Eilbeck J C, Lomdahl P S and Scott A C 1984 *Phys. Rev.* B **30** 4703
[5] Davydov A S 1980 *Zh. Eksp. Teor. Fiz.* **78** 789 (Engl. Transl. 1980 *Sov. Phys.–JETP* **51** 397
[6] Halding J and Lomdahl P S 1987 *Phys. Lett.* **124A** 37
[7] Lomdahl P S and Kerr W C 1985 *Phys. Rev. Lett.* **55** 1235
[8] Lawrence A F, McDaniel J C, Chang D B, Pierce B M and Birge R R 1986 *Phys. Rev.* A **33** 1188
[9] Bolterauer H 1986 *Structure, Coherence, and Chaos Proc. MIDIT Workshop (1986)* (Manchester: Manchester University Press)
[10] Cruzeiro L, Halding J, Christiansen P L, Skovgaard O and Scott A C 1988 *Phys. Rev.* A **37** 880
[11] Cottingham J P and Schweitzer J W 1989 *Phys. Rev. Lett.* **62** 1792
[12] Wang X, Brown D W and Lindenberg K 1989 *Phys. Rev. Lett.* **62** 1796
[13] Motschmann H, Förner W and Ladik J 1989 *J. Phys.: Condens. Matter* **1** 5083
[14] Förner W and Ladik J 1990 *Proc. MIDIT Workshop, (Hanstholm, 1989)* (New York: Plenum)
[15] Scott A C 1982 *Phys. Rev.* A **26** 578; 1983 *Structure and Dynamics: Nucleic Acids and Proteins* ed E Clementi and R H Sarma (New York: Adenine) p 389; 1984 *Phys. Scr.* **29** 279; 1985 *Phil. Trans. R. Soc.* A **315** 423
MacNeil L and Scott A C 1984 *Phys. Scr.* **29** 284
[16] Nevskaya N A and Chirgadze Y N 1976 *Biopolymers* **15** 637

[17] Hamilton W C and Ibers J A 1968 *Hydrogen Bonding in Solids* (New York: W A Benjamin)
[18] Novak A 1974 *Struct. Bonding (Berlin)* **18**
[19] Kuprievich V A and Klymenko V W 1977 *Mol. Phys.* **34** 1287
[20] Kerr W C and Lomdahl P S 1987 *Phys. Rev.* B **35** 3629
[21] Kerr W C and Lomdahl P S 1990 *Proc. MIDIT Workshop (Hanstholm, 1989)* (New York: Plenum)
[22] Mechtly B and Shaw P B 1988 *Phys. Rev.* B **38** 3075
[23] Skrinjar M J, Kapor D V and Stojanovic S D 1988 *Phys. Rev.* A **38** 6402; 1989 *Phys. Rev.* B **40** 1984
[24] Brown D W, Lindenberg K and West B J 1986 *Phys. Rev.* A **33** 4104
Brown D W, West B J and Lindenberg K 1986 *Phys. Rev.* A **33** 4110
Brown D W 1988 *Phys. Rev.* A **37** 5010
[25] Brown D W, Lindenberg K and West B J 1987 *Phys. Rev.* B **35** 6169
[26] Brown D W, Lindenberg K and West B J 1988 *Phys. Rev.* B **37** 2946
[27] Brown D W and Ivic Z 1989 *Phys. Rev.* B **40** 9876
[28] Förner W 1991 *J. Comput. Chem.* submitted
[29] Scott A C 1991 *Proc. Conf. on Nonlinear Sciences: The Next Deal (Los Alamos National Laboratory, 21 May 1990)*
[30] Brizhik L, Gaididei Yu B, Vakhnenko A A and Vakhnenko V A 1988 *Phys. Status Solidi* b **146** 605
[31] Lomdahl P S and Kerr W C 1990 *Proc. MIDIT Workshop (Hanstholm, 1989)* (New York: Plenum)
[32] Itoh K and Shimanouchi T 1972 *J. Mol. Spectrosc.* **42** 86
[33] Pierce B M 1990 *Proc. MIDIT Workshop (Hanstholm, 1989)* (New York: Plenum)